Nigerian Journal of Engineering, Vol. 29, No. 3, December 2022, ISSN (print): 0794 – 4756, ISSN(online):2705-3954.

Nigerian Journal of Engineering,
Faculty of Engineering, Ahmadu Bello University, Zaria, Nigeria
journal homepage: www.njeabu.com.ng

Modeling and Implementation of a Self-Tuning Adaptive Controller of an Inverter in a Grid-Connected Microgrid

M. S. Hassan*, A. S. Abubakar, S. Salisu, A. J. Aliyu, M.D. Almustapha

Department of Electrical Engineering, Ahmadu Bello University, Zaria – Nigeria
*sanimubashirabu@yahoo.com,

Research Article

Abstract

The grid system has become more intelligent to enable the flow of electricity in a reliable and steady manner due to the consequences of unceasing penetration of distributed renewable energy generation. This can be done by doing smart decisions such as replacing the outdated component of the conventional inverter with the more effective and recently developing components such as the Self-tuning adaptive controller. This paper presents a control strategy by incorporating an adaptive self-tuning controller into the conventional model. The controller developed is based on Recursive Least Square Algorithm (RLSA) with variable pole shifting control and was then implemented on the Grid Connected Inverter. The conventional PI controller in the inner current control loop and outer voltage control loop of the conventional model were replaced and comparison between the two different controllers (Proportional Integral controller and Self-Tuning controller) was carried out. The model was simulated on MATLAB Simulink interface. Performance analysis of inverter controller and change in grid filter inductance were studied and all the result showed that ST controller have a better system response and a better performance than when PI controller is used. The grid voltage showed a 1.15% THD when using ST controller and 1.36% THD when using PI controller which resulted to 18.26% reduction in THD. The injected current shows a 1.31% THD and 1.21% when using PI and ST controller respectively.

Keywords
Adaptive control; Pole shifting controller; RLS Algorithm; Self-tuning controller.

Article History
Received: – September, 2022 **Accepted: –** December, 2022
Reviewed: – November, 2022 **Published: –** December, 2022

1. Introduction

The effect of continuous penetration of intermittent, distributed renewable energy generation has made it a necessity for the grid system to become more intelligent to enable the flow of electricity in a reliable and steady manner. In practice, the dynamics of the grid system may not fully be understood and their parameters may vary over time. To cope with this challenging issue, modern control systems need to satisfy a certain degree of robustness and adaptability (Anavatti *et al* 2016).

The grid system requires advanced systems to monitor the voltage and current regulation unlike the past where grid-tied inverters disconnect during strange grid conditions or faults, and wait for normal grid conditions to reconnect.

Various studies have been conducted to overcome the short-comings of the standard vector control approach which uses fixed gain PI controllers. An adaptive control approach was proposed which employs a direct current control (DCC) strategy (Li *et al.*, 2011). Another method uses intelligent control principles to reduce the error between the desired and actual d- and q-axis currents through an adaptive tuning process (Wang *et al.*, 2018). A predictive current control was presented by Espi *et al.* (2011) but the controller becomes unstable if the programmed filter inductance becomes different from its actual value or if there is an inaccuracy in measurement.

The conventional control has some drawbacks which include high overshoot when starting, sensitivity to controller gains and slow response when there is sudden disturbance. It was found that the conventional approach is also sensitive to model uncertainties (Dannehl *et al.*, 2009).

To overcome the shortcomings of the conventional controllers, adaptive controllers were developed. The non-adaptive (fixed-parameter) controller is, in general, based on one particular system operating condition. The key disadvantage of the non-adaptive controller is that there is the possibility of the controller performance deteriorate under other operating conditions.

The parameters of the controller must be re-tuned in some situations where broad dispersion of the system parameters is expected (Figueres *et al.*, 2009). Furthermore, it is not possible to achieve maximum performance for each and every operating condition when the controller parameters are fixed. Hence, adaptive control techniques have been proposed to overcome the disadvantage of fixed-parameter controller design. In this adaptive controller design presented, the controller parameters are determined online and adaptive to the changes that may occur in system operating conditions (Gianto., 2015).

The aim of this paper is to model and implement a self-tuning adaptive controller of an inverter in a grid-tied micro-grid. This research showed how such restriction can be overcome by using an adaptive self-tuning controller instead of a PI controller. A controller based on recursive least squares identification and pole shifting control was designed and implemented on the grid connected inverter (GCI). The proposed controller showed robust and stable performance for a wide range of operating conditions.

2. Self-Tuning Controller (STC)

Self-tuning controller (STC) of adaptive control theory can be described as one of the techniques of adaptive control whereby the adaptation controller is developed so as to overcome the various limitations of the non-adaptive controllers. The non-adaptive (fixed-parameter) controller is normally supported by one specific system operational condition. One of the disadvantages of the non-adaptive controller is that the performance is not optimal at conditions other than the ideal condition. Adaptation control techniques are recently arranged in order to overcome the various disadvantages of the fixed-parameter controller design such as taking longer to converge and a longer response time. In this adaptation controller style, the controller parameters are determined on-line and adaptation to the dynamics in system operational conditions (Gianto., 2015). Figure 1 shows the block diagram of the self-tuning controller.

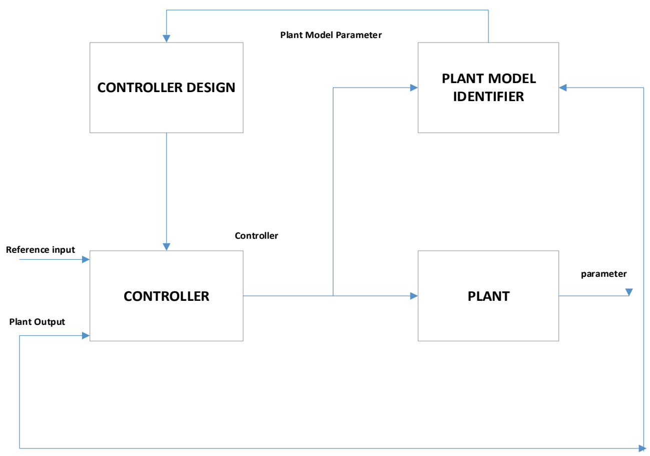

Figure 1: Self Tuning Controller (Shakeel *et al.*, 2020)

3. Methodology

3.1 Self-tuning Adaptive Controller implementation in a grid connected system

To implement the ST adaptive controller for the grid connected inverter in the proposed micro-grid, the inner current loop controller and the outer voltage loop controller are replaced with self-tuning controllers. These ST controllers uses Recursive Least Square algorithm and variable forgetting factor for the parameter estimation and pole shifting control to adapt and identify suitable system parameters in real-time.

The design of the proposed STC controller is summarized by the flowchart in Figure 2.

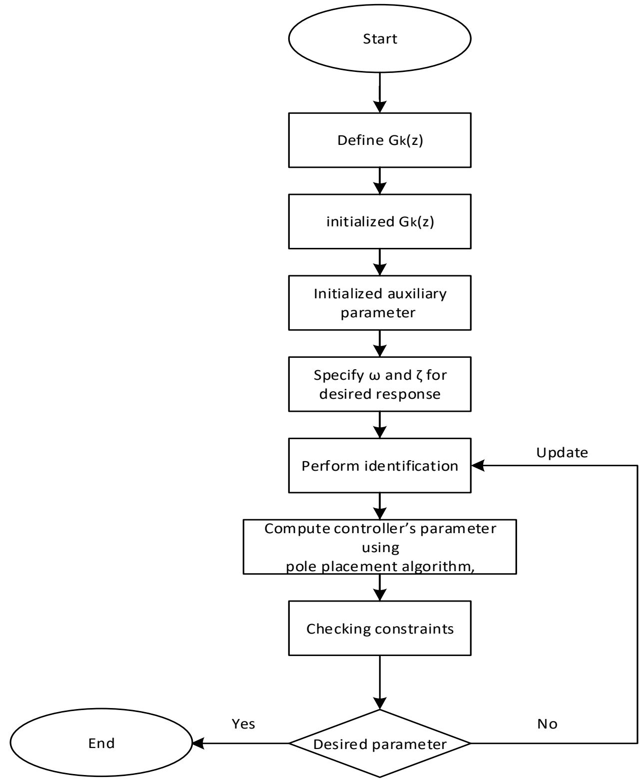

Figure 2: Flow chart for Self-tuning controller design

Where G_K is the gain and is given as;

$$G_K(z^{-1}) = \frac{q_0+q_1z^{-1}+q_2z^{-2}+q_3z^{-3}}{1+(p_1-1)z^{-1}+(p_1+p_2)z^{-2}+(-p_2)z^{-3}} \tag{1}$$

The auxiliary parameters are φ, λ, ρ and η, where φ is the forgetting coefficient, η is the efficiency λ is the discrete transfer function. These parameters are defined in the equations (2) to (6).

$$\varphi_k = \frac{1}{a+(1+\rho)\left\{\ln(1+\xi)+\left[\frac{(v_k+1)\eta}{1+\xi+\eta}-1\right]\frac{\xi}{1+\xi}\right\}} \tag{2}$$

$$\eta = \frac{\left(y_k-\theta_{k-1}^T\phi_k\right)^2}{\lambda_k} \tag{3}$$

$$\lambda_k = \varphi_{k-1}\left[\lambda_{k-1} + \frac{\left(y_k-\theta_{k-1}^T\phi_k\right)^2}{1+\xi}\right] \tag{4}$$

C_k is the covariance matrix and is defined as;

$$C_k = C_{k-1} - \frac{C_{k-1}\cdot\phi_k\cdot\phi_k^T\cdot C_{k-1}}{\varepsilon^{-1}+\xi} \tag{5}$$

$$\xi = \phi_k^T \cdot C_{k-1} \cdot \phi_k \tag{6}$$

Wherey_k is the system output andϕ_k is the predicted process output (Mansor et al. 2011).

3.2 Implementation of the Recursive Least Square (RLS) Algorithm

The choice for choosing RLS algorithm is due to the fact that it is one of the simplest on-line identification methods which require less computation time when compared to others and also because the algorithm has a good numerical stability and a fast convergence property.

In STC, the model of the system to be controlled is usually expressed with a linear difference equation and the given model parameters are analyzed every sampling interval. Considering the discrete-time domain, the system model is assumed to be;

$$y(n) + h_1 y(n-I) + h_2 y(n-2) + \cdots + h_{n_h} y(n-n_h) = b_0 u(n) + b_1 u(n-I) + b_2 u(n-2) + \cdots + b_{n_b} u(n-n_b) \quad (7)$$
$$+\varepsilon(n) + g_l \varepsilon(n-I) + g_2 \varepsilon(n-2) + \cdots + g_{n_g} \varepsilon(n-n_g)$$

Where; y is the plant output, u is the input, h_i and b_i are the model parameters identified, ε is a sequence of independent and equally distributed random noise, n is the number of sampling instants.

Let the backward shift (or delay) operator beq^{-1}, which is used to relate to equation 8 (Chalam 1987).

$$q^{-k} y(n) = y(n-k) \quad (8)$$

On using equation 8 above, it can be written as;

$$H(q^{-1}) y(n) = B(q^{-I}) u(n) + G(q^{-1}) \varepsilon(n) \quad (9)$$

Where;

$$H(q^{-1}) = 1 + h_1 q^{-1} + h_2 q^{-2} + \cdots + h_{n_h} q^{-n_h}$$
$$B(q^{-1}) = b_0 + b_1 q^{-1} + b_2 q^{-2} + \cdots + b_{n_b} q^{-n_b} \quad (10)$$
$$G(q^{-1}) = I + g_1 q^{-1} + g_2 q^{-2} + \cdots + g_{n_g} q^{-n_g}$$

The analysis of the given model parameters can be simplified by assuming Gq^{-1}= 1, which modifies (10) to become;

$$H(q^{-1}) y(n) = B(q^{-1}) u(n) + \varepsilon(n) \quad (11)$$

In terms of the numerous model parameters, Equation 11 can be given as (12);

$$y(n) + h_l y(n-I) + h_2 y(n-2) + \cdots + h_{n_h} y(n-n_h) = b_0 u(n) + b_l u(n-I) + b_2 u(n-2) + \cdots + b_{n_b} u(n-n_b) + \varepsilon(n) \quad (12)$$

By introducing the parameter and regression vectors;

$$\mathbf{\Theta}(n) = [h_1 \quad h_2 \quad \cdots \quad h_{n_h} \quad b_0 \quad b_1 \quad \cdots \quad b_{n_b}]^T \quad (13)$$

In a compact form, Equation 12 can be rewritten, using definition in the equation to form (14)

$$y(n) = \Phi(n)^T \Theta(n) + \varepsilon(n) \quad (14)$$

Therefore, the parameter vector ($\mathbf{\Theta}$)will be analyzed from the observations of the system inputs and outputs. The parameters of adaptive controllers are obtained sequentially in real time which is needed to minimize the computation time. Evaluation of the least-squares estimate is arranged in such a way that the outcome obtained at time *n-1* can be used to get the result at time *n*. In recursive implementations of the least-squares method, the computation is initialized with already known initial conditions, and then the information contained in the new data samples gotten from the measurements are used to update the old estimates.

3.3 Implementation of Pole Shifting Controller

In the pole-shifting controller design, the pole characteristic polynomial of the closed-loop system is required to be obtaining the same computation which is in the same order with the pole characteristic polynomial of the open-loop system. However, the pole locations determined by the roots of the characteristic polynomial are shifted by a factor α_s.

The closed-loop system poles (the position of the poles of a closed loop transfer function) are shifted towards the center of the unit circle in the z-domain by a given factor α which is less than 1 as shown in the Figure 3. For a small pole shift, a small control output will be desired to actualize small increase in stability margin in the system, Whereas, the controller is driven to reach its limits due to a large pole shift.

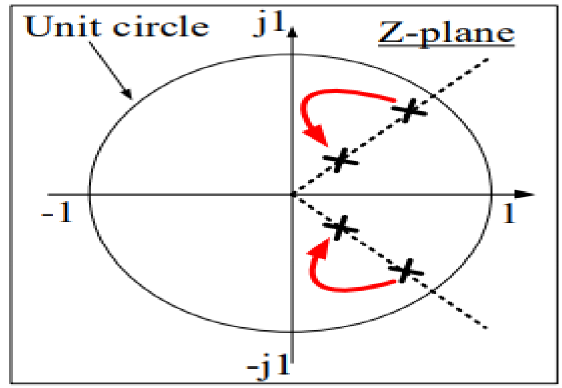

Figure 3: Pole Shifting Process

The computational procedures that are used for deriving the pole shifting control is given in equation 15 to 19. Assuming that the feedback loop has the form;

$$\frac{u(t)}{y(t)} = -\frac{G(z^{-1})}{F(z^{-1})} \quad (15)$$

Where;

$$F(z^{-1}) = 1 + f_1 z^{-1} + f_2 z^{-2} + \cdots\cdots + n_f z^{-n_f} \quad (16)$$
$$G(z^{-1}) = g_0 + g_1 z^{-1} + g_2 z^{-2} + \cdots\cdots + n_g z^{-n_g} \quad (17)$$

And $n_f = n_b - 1, n_g = n_a - 1$,therefore, the characteristic equation of the closed loop system can be computed as:

$$T(z^{-1}) = A(z^{-1}) F(z^{-1}) + B(z^{-1}) G(z^{-1}) \quad (18)$$

The pole-shifting algorithm transform$T(z^{-1})$to take the form of $A(z^{-1})$, but considering the pole locations that is shifted by a factor α, it becomes eqn. 19;

$$A(z^{-1}) F(z^{-1}) + B(z^{-1}) G(z^{-1}) = A(\alpha z^{-1}) \quad (19)$$

3.4 Simulation Parameters

Table 1 shows the simulation parameters. These parameters were adopted from the work of Shakeel & Malik (2020).

Table 1: Simulation parameters

PI Controller for GCI		
Controller	K_p	K_i
D-axis current controller	0.3	20
Q-axis	0.3	20
Dc-link voltage (V)	7	800
Grid Parameter	**Value**	
Supply frequency	60Hz	
Three short circuit level at base voltage	2,500MVA	
Base Voltage (Line to Line RMS value)	120 x 10^3V	
X/R ratio	7	
Substation transformer	47MVA 120KV/25KV	

4. Simulation Result

4.1 Performance Analysis of Inverter Controller

The inverter controller entails a nested loop control structure in the dq synchronous reference frame with outer voltage loops and inner current loops. The dc voltage (V_{dc}) is regulated by the outer voltage d-axis control loop which generates the reference current value for the inner current loop makes the d-axis current follow and control the active power transfer between the inverter and micro-grid.

From the result obtained on Figure 4, It can be noticed that the PI and ST controllers were able to regulate the dc bus voltage towards its reference value of 1500V during the operation. However, the ST controller is observed to show a better transient performance with less overshoot and settling time during the sudden change.

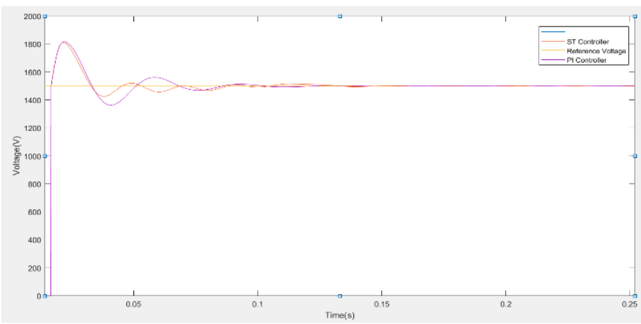

Figure 4: DC bus-voltage variation during step load change

4.2 Change in Grid Filter Inductance

To inspect the robustness (the ability of a system to withstand parameter variations in a plant transfer function) of the controller during system parameter changes, the modeling inductance was varied to achieve the differences. The modeling inductance was gradually increased during the system operating condition until a noticeable variation were noticed in the system response. The variation in grid injected current when a disturbance is introduced is shown in Figure 5. It can be noticed that the PI controller deteriorate in the first 0.15s whereas the ST controller is able to adapt and maintain an optimal performance.

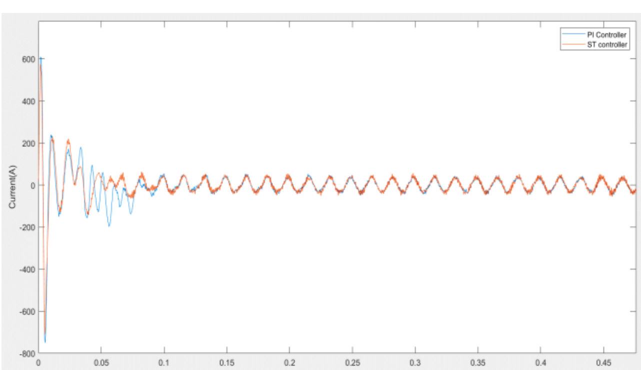

Figure 5: Variation of injected current during system parameter changes

4.3 Harmonic Analysis of the Grid-Injected Current and Grid Voltage

The composition and control approaches of the grid-tied inverter can affect the harmonics level of the injected current and voltage in the system. According to IEEE standards 1547 and 519, it is suggested that the overall THD at the point of common coupling should be less than 5% either for current total harmonics distortion or voltage total harmonics distortion. Fast Fourier transform (FFT) analysis was carried out to record each harmonic and to compute the THD of the grid connected inverter output waveforms (current and voltage) at PCC. The harmonic analysis was done for up to 50th order harmonics and the results are presented in Figure 6 to 9.

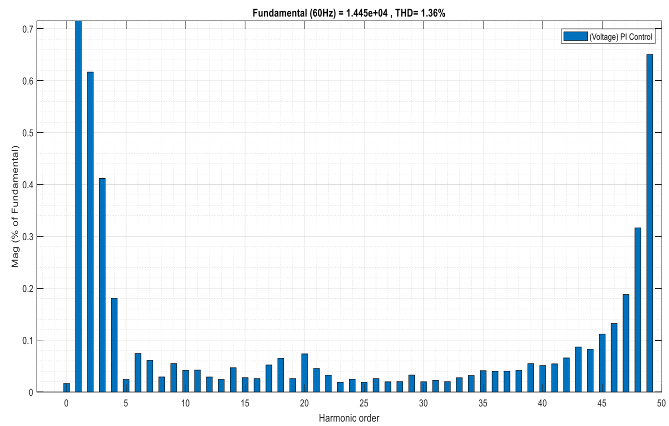

Figure 6: THD of the grid voltage when PI controller is used

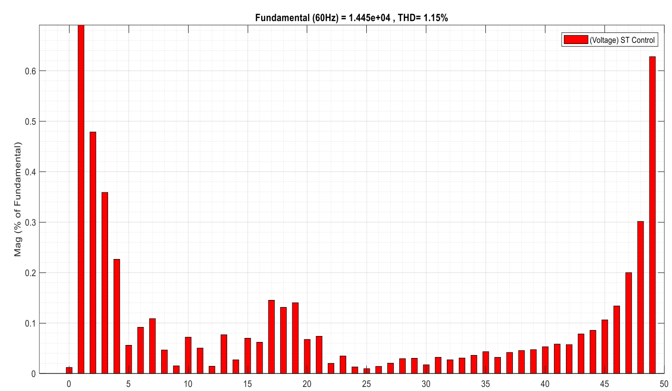

Figure 7: THD of the grid voltage when ST controller is used

The analysis shows that both the PI and ST controllers were able to maintain the IEEE standard when studying the harmonic spectrum of the grid voltage, however, the ST controller perform better with the Total Harmonic Distortion of 1.15% as shown in Figure 7 and a Total Harmonic Distortion when using the PI controller to be 1.36% as shown in Figure 6, given a 18.26% reduction in THD.

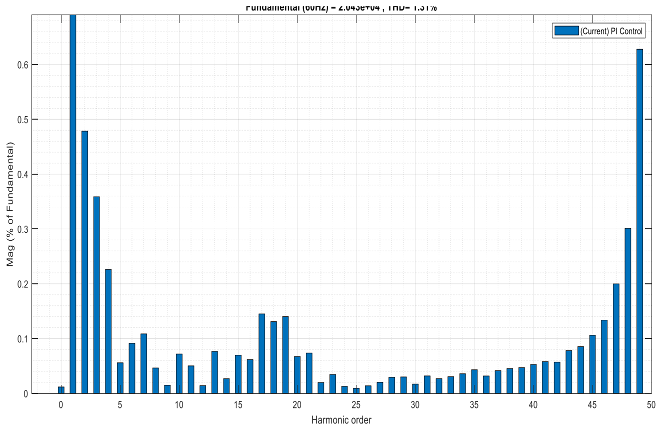

Figure 8: THD of the grid injected current with PI controller

Figure 9 shows that the self-tuning controller also produces lesser current distortions. The analysis shows that there is a 1.31% THD when using the PI controller as shown in Figure 8 as against a 1.21% THD when using the ST controller as shown in Figure 9, giving an 8.26% decrease in THD. The study shows that the designed systems with both PI and ST controller adhere to the harmonic standards by limiting the THD below 5% and shows that an improved power quality is obtained for the distributed generation system when ST controller is used.

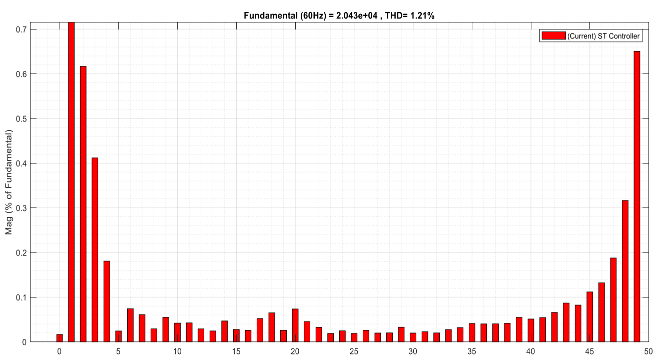

Figure 9: THD of the grid injected current with PI controller

5. Conclusion

This research has presented the development of a self-tuning (ST) adaptive controller of an inverter in a grid connected micro-grid which shows a better performance than the conventional proportional-integral (PI) controller. The simulation analysis shows that the ST controller have a better transient response and settling time as compared to PI controller. The change in grid current shows that the grid current deteriorates at a certain period of time when using the PI controller but was able to adapt and maintain an optimal performance even after the introduction of disturbance when using the ST controller. The harmonic analysis of the grid-injected current and grid voltage was also studied, it shows that an improvement in THD of 18.26% at grid voltage and 8.26% improvement at the injected current was discovered when comparing the two controllers.

References

Anavatti, Sreenatha G., Fendy Santoso, and Matthew A. Garratt. 2016. "Progress in Adaptive Control Systems: Past, Present, and Future." (October): 1–8.

Chalam, V V. 1987. *Adaptive Control Systems: Techniques and Applications*. USA: Marcel Dekker, Inc.

Dannehl, J, C Wessels, and F W Fuchs. 2009. "Limitations of Voltage-Oriented PI Current Control of Grid-Connected PWM Rectifiers With LCL Filters." *IEEE Transactions on Industrial Electronics* 56(2): 380–88.

Figueres, E et al. 2009. "Sensitivity Study of the Dynamics of Three-Phase PV Inverters With an LCL Grid Filter." *IEEE Transactions on Industrial Electronics* 56(3): 706–17.

Gianto, Rudy. 2015. "Review Of Self-Tuning Controller And Its Application In Electrical Power System." *Review Of Self-Tuning Controller And Its Application In Electrical Power System* 4(11): 137–42.

Li, Shuhui, Timothy A Haskew, Yang-Ki Hong, and Ling Xu. 2011. "Direct-Current Vector Control of Three-Phase Grid-Connected Rectifier–Inverter." *Electric Power Systems Research* 81(2): 357–66. http://www.sciencedirect.com/science/article/pii/S037877961000221X.

Mansor, H, Samsul Noor, Raja Kamil, and Farah Saleena Taip. 2011. "Online Quantitative Feedback Theory (QFT) - Based Self- Tuning Controller for Grain Drying Process." (August 2014).

Paál, E., Z. Weitzl, and C. S. Choi. 2011. "Grid Management Functions Built in PV Inverters for Distributed Power Generation." *8th International Conference on Power Electronics - ECCE Asia: "Green World with Power Electronics", ICPE 2011-ECCE Asia*: 2637–44.

Shakeel, Femina M., and Om P. Malik. 2020. "On-Line Self-Tuning Adaptive Control of an Inverter in a Grid-Tied Micro-Grid." *Electric Power Systems Research* 178(October 2019).

Vasquez, J C 2009. "Adaptive Droop Control Applied to a VSI Operating in Grid-Connected and Islanded Modes." *IEEE Transactions on Industrial Electronics* 56(10): 4088–96.

Wang, Yahui 2018. "Hybrid AC/DC Microgrid Architecture with Comprehensive Control Strategy for Energy Management of Smart Building." *International Journal of Electrical Power & Energy Systems* 101: 151–61.